Influence of Nonlinearities on the Vertical Kinematic Interaction of Piles

Usama Zafar[1], Chandra S. Goit[1], Masato Saitoh[1]
[1]Saitama University
255 Shimo-Okubo, Saitama, Japan
uzcivil@gmail.com; chandra@mail.saitama-u.ac.jp; saity@mail.saitama-u.ac.jp

Abstract - Numerical investigations to obtain the kinematic response of piles in soil under vertical dynamic loading using three-dimensional finite element modelling were carried out in the time domain. A numerical model was validated against the available solutions for end-bearing single piles. Based on this validation, the model for floating single pile was developed. Besides the elastic assumptions for soil, the effects of soil and soil-pile interface nonlinearities on the kinematic response of piles were examined. The results show that the kinematic response factors of the end-bearing single pile and floating single pile based on elastic soil match well with the available analytical/numerical solutions. The assumption of the insignificance of the soil-pile interface may hold true for end-bearing single pile with elastic soil consideration. Whereas both in cases of end-bearing single pile and floating single pile, with consideration for soil nonlinearity and the soil-pile interface nonlinearity, the kinematic interaction can increase reasonably considering piles can move easily against relatively weaker soil.

Keywords: Kinematic interaction, Numerical simulation, Vertical loading, Soil nonlinearity

1. Introduction

Soil-pile-structure interaction is typically considered in the structural design using the sub-structuring approach [1, 2] wherein inertial and kinematic interactions are determined separately. During seismic excitation, kinematic interaction that causes a difference in the movement of piles and the surrounding soil as a result of stiffness contrast between the two has been a subject of immense interest [3-7]. It is noteworthy that most of the available studies focus on the lateral ground excitations; kinematic interactions under vertical ground motions are generally ignored assuming it as a conservative design approach [8, 9]. However, neglecting the role of vertical kinematic interaction despite knowing the site-specific characteristics and possible damaging effect of vertical ground motions, as reported in some recent earthquakes, can be misleading [10]. Additionally, over-conservative design practices for structures are being discouraged all over the world with the emergence of performance-based design strategies. Mindful of all, it is of significance to understand the influence of modified ground motion on the response of pile foundations by kinematic interaction.

A range of work has been carried out for the vertical kinematic interaction of piles in recent years. Some of these studies have utilised boundary element methods to estimate the pile response [11, 12] while others have considered the spring and dashpot system for soil and pile [8, 9]. Additionally, studies based on numerical approaches are equally available. Anoyatis et al. [8] employed the finite element approach in the frequency domain to validate the proposed elastodynamic model. Most of these analytical and numerical approaches, however, assume soil to be linear elastic/viscoelastic in obtaining the kinematic response. It is well known that soil exhibits nonlinear behaviour when subjected to intense loading conditions. Besides, these studies do not consider the interface between the soil and the pile, although, piles may slip against the soil due to the difference in relative soil-pile movement.

The current study employs nonlinear three-dimensional finite element modelling to quantify vertical kinematic interactions in the time-domain. Both the elastic and inelastic behaviours of soil are considered. Additionally, the frictional interface between the soil and pile is considered to account for the possible slip of piles against the soil. Firstly, an end-bearing single pile model is validated against the available analytical results for end-bearing single piles. The approach is then extended to floating single piles. Results are obtained in the form of kinematic response factors and amplification ratios.

2. Numerical Modelling For Soil-Pile

Three-dimensional finite element modelling was carried out using commercially available software PLAXIS 3D v.21.01 [13]. Table 1 shows three different simulation cases considered in this study for variations in model size, pile configuration, and pile tip. In the table, Ep and Es are Young's modulus of elasticities of pile and soil, respectively; L is the length of the pile; d is the pile diameter; and H is the soil height.

Table 1: Types of numerical simulation cases.

Simulation run case	Modulus ratio	Slenderness ratio	Soil height by length ratio	Pile configuration	Pile tip condition
-	(E_p/E_s)	(L/d)	(H/L)	-	-
RC-1	100	25	1	Single pile	End-bearing
RC-2	100	20	2	Single pile	Floating

2.1. Validation using an end-bearing single pile

The numerical model used for the end-bearing single pile (RC-1) is presented in Fig. 1. Only the half symmetry was considered to decrease the computational time. The lateral dimension of 200 times the diameter of the pile (d) was used to get proper attenuation of dynamic waves of soil without any reflection near the boundaries (after Anoyatis et al. [8]). Additionally, free-field boundaries were used. The vertical dimension of soil was selected equal to the pile length to have the same boundary conditions at the pile tip and soil base. The sides of the soil were laterally constrained to enable only vertical translation. Two kinds of models were established: one with joined nodes between soil and pile and the other having separated nodes to check the effect of the soil-pile interface. To mesh three-dimensional volumes of soil and pile, four-node tetrahedral linear elements were used. The minimum element size was selected such as to avoid any hindrance in the propagation of dynamic waves.

Vertical dynamic loading in the form of unit harmonic acceleration (1 m/s2) for a wide frequency range (0.5 Hz to 36 Hz) was applied at the soil base and tip of the end-bearing single pile. Transient dynamic analysis was performed to consider the effects of soil and soil-pile interface nonlinearities. Four kinds of analysis were performed for RC-1 considering: (a) elastic soil, (b) elastic soil and soil-pile interface, (c) nonlinear soil, and (d) both soil and soil-pile interface nonlinearities.

For soil, properties of Gifu sand [2] were used. Soil nonlinearity was incorporated in the models through Mohr-Coulomb (MC) failure criteria; MC yielding criterion was used for the frictional soil-pile interface. The properties considered for the soil and soil-pile interface are listed in Table 2. Young's modulus of soil (Es) was determined using the values of shear wave velocity, density, and Poisson's ratio of the soil. Besides, the shear strength parameters were deduced using triaxial test data of the soil. For the soil-pile interface, the material strength of interface was reduced two-thirds times the strength of soil, as conventionally taken for cohesionless soil [2]. Moreover, 5% Rayleigh damping was considered in all analyses.
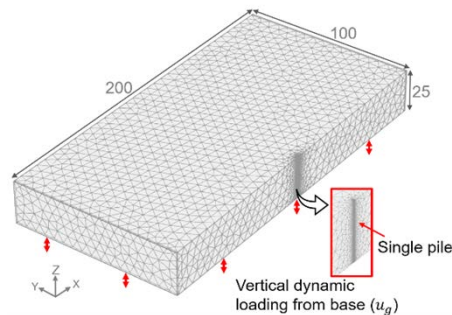

Fig. 1: Numerical model for RC-1: end-bearing single pile (all dimensions are in "m").

Table 2: Parameters used for Mohr-Coulomb model and soil-pile interface

Parameter	Symbol	Value	Units
Young's modulus of soil	E_s	148,200	kPa
Shear wave velocity of soil	V_s	171.5	m/s
Compressional wave velocity of soil	V_p	420.1	m/s
Density of soil	ρ_s	17.6	kN/m^3
Poisson's ratio of soil	v_s	0.4	-
Friction angle of soil	φ'	40.7	Degrees
Cohesion of soil	c	1	kPa
Dilatancy angle of soil	ψ	10.7	Degrees
Interface to soil material ratio	R_{inter}	0.67	-

The resulting absolute kinematic response factors ($|\,I_v\,|$) for case RC-1 determined by dividing the oscillation at the pile top to that at the soil surface, are shown in Fig. 2. The values are plotted against the dimensionless frequency ratio (ω/ω_1), where ω is the angular frequency and ω_1 is the first resonant frequency determined as

$$\omega_1 = \frac{V_p \pi}{2H} \tag{1}$$

where V_p is compressional wave velocity of soil and H is the height of the soil domain. By Eq. (1), $\omega_1 = 26.4$ rad s^{-1}.

It can be seen from Fig. 2 that $|\,I_v\,|$ agree well with the finite element-based solution by Anoyatis et al. [8] and analytical-based solution by Dai et al. [11] in the entire frequency range. In the range of $\omega/\omega_1 = 0$ through $\omega/\omega_1 = 0.3$, the close to the static response of pile can be seen as $|\,I_v\,|$ become close to one; the pile moves together with the soil. Close to the resonant frequency ($\omega/\omega_1 = 1$), a slight variation in $|\,I_v\,|$ can be noticed in the zoomed view, highlighting possible amplification of soil surface movement at the resonant frequency.

With the increase in loading frequency, the kinematic response factors begin to decrease until around $\omega/\omega_1 = 3.5$. This results from the difference in the vibration response of the stiffer pile and softer soil against higher frequency components of the incident vertical dynamic wave also termed as filtering effect kinematic interaction. Beyond this dimensionless frequency ratio, the fluctuating pattern of $|\,I_v\,|$ can be observed.
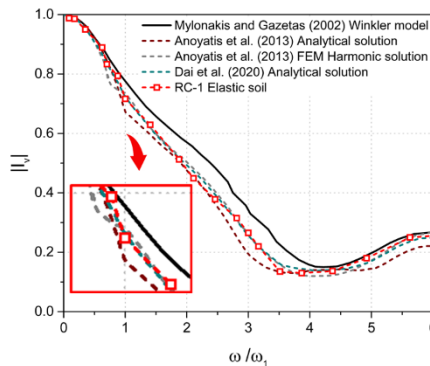

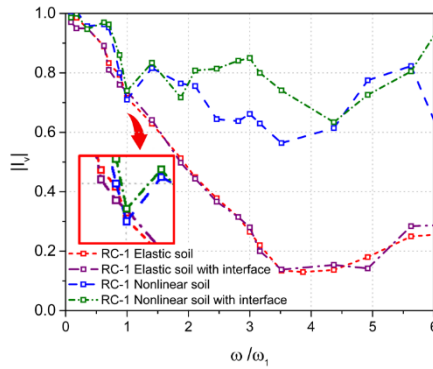Fig. 2: Kinematic response factor for end-bearing single pile.

Fig. 3: Kinematic response factor for end-bearing single pile: comparison of elastic soil with soil and soil-pile interface nonlinearities.

In Fig. 3, the comparison among kinematic interactions for case RC-1 based on elastic soil, elastic soil with the soil-pile interface, nonlinear soil only, and nonlinear soil with the soil-pile interface is presented. It is evident that for elastic soil with the soil-pile interface, the values are comparable to the ones by elastic soil only. As with the incident vertical dynamic wave acting at pile tip and soil base, the pile is not able to show any change in response even with its independent nodes from the surrounding elastic soil than with joined nodes.

With consideration of soil nonlinearity, a significant increase in overall $| I_v |$ can be seen. According to the amplification ratio data of pile top and soil surface (explained in the ensuing paragraph), less restriction against pile movement is offered by the nonlinear soil around the pile shaft. Besides, the soil surface movement may decrease with nonlinearity. Hence, these changes in movements of pile top and soil surface increases the values of $| I_v |$. While at $\omega/\omega_1 = 1$, a noticeable decrease in $| I_v |$ can be observed at the first frequency resulting from the amplification of soil surface at resonant frequency (discussed in the subsequent paragraph). Moreover, consideration of soil and soil-pile interface nonlinearities change the pile response prominently when compared with soil nonlinearity only case. It stems mainly from the fact that the pile faces weaker restrictions relying on the frictional contact with soil and hence, can slide easily. Additionally, the decrease in the soil surface motion with nonlinear properties can further increase the values of $| I_v |$. Besides, at the first resonant frequency, the decrease in $| I_v |$ occurs analogous to other cases.

The absolute ratios of the vertical motions applied at the pile top to those at the soil base termed as amplification ratio ($| A |$) are shown in Fig. 4. Results show that the maximum amplification ratio of around 7 appears at the first resonant frequency of soil (i.e., at $\omega/\omega_1 = 1$). It can be noticed that the amplification ratios of the pile using elastic soil with/without the soil-pile interface are analogous.
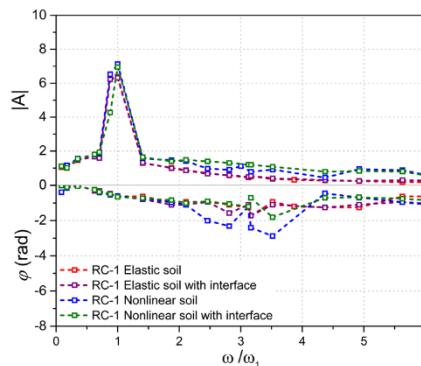

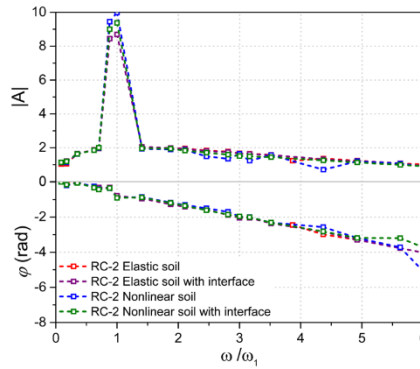Fig. 4: Amplification ratio and corresponding phase at pile-top of end-bearing pile.

Fig. 5: Amplification ratio and corresponding phase at soil surface of end-bearing single pile.

With nonlinear soil only and both soil and soil-pile interface nonlinearities, the amplification ratios can increase noticeably than the elastic ones during higher frequency ratios ($> \omega/\omega_1 = 1$). This results from the ease in vertical movement of the pile with soil/soil-pile interface nonlinearities (as discussed earlier). Moreover, the phase differences between the oscillations of pile top and soil base show that the slight variation occurs at $\omega/\omega_1 = 1$. The values increase till $\omega/\omega_1 = 3.5$, showing the filtering effect of the higher frequency components of the vertical dynamic waves.

The amplification ratios ($| A |$) and equivalent phase differences (ϕ) at soil surface for case RC-1 are presented in Fig. 5. The maximum amplification at the first resonant frequency can be noticed for each analysis. Beyond this frequency, the decreasing trend of the values occurs. In comparison to Fig. 4, it is evident that the soil surface and pile top show analogous values at lower frequencies, while with the increase in frequencies, the difference in values keeps increasing. Besides, it can also be observed that $| A |$ at the soil surface decrease slightly with the consideration of nonlinearities.

Also, it can be observed in Fig. 5 that ϕ at the soil surface tend to increase with the increase in loading frequency resulting from the change in vibrating mode of soil after the first resonant frequency. On the contrary, the changes in ϕ at the pile top are insignificant in higher frequencies (Fig. 4), as it is difficult for the pile to move following the soil movement due to its higher stiffness.

2.2. Numerical modelling of floating single pile

Based on the validation of the end-bearing single pile, the same numerical methodology was employed for the floating single pile in RC-2. As indicated in Table 1, the height of the soil domain is kept twice the length of the pile. Whereas the lateral dimensions were kept the same (200×100) as in RC-1. The same free-field boundaries were used in lateral directions. Besides, the same vertical dynamic loading, as explained in section 2.1 was applied from the soil base.
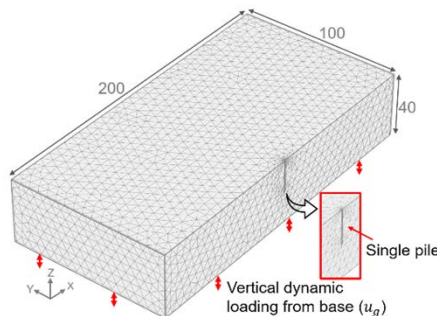

Fig. 6: Numerical model for RC-2: floating single pile (all dimensions are in "m").
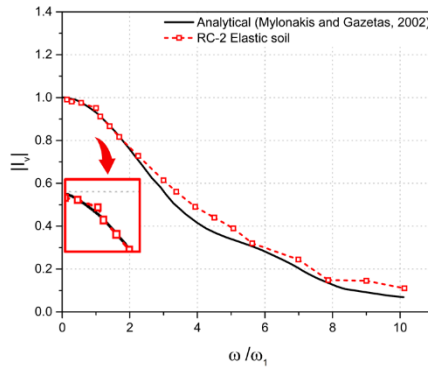
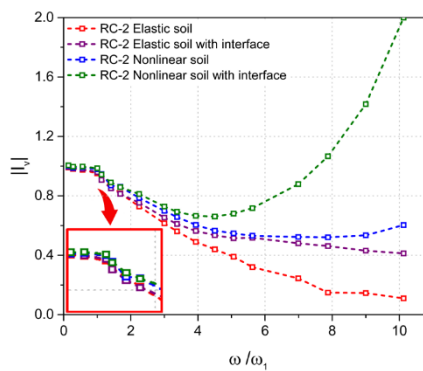Fig. 7: Kinematic response factor for floating single pile.

Fig. 8: Kinematic response factor for floating single pile: comparison of elastic soil with soil and soil-pile interface nonlinearities.

The results presented in Fig. 7 shows the attained absolute kinematic response factors ($| I_v |$) for case RC-2 for the elastic soil conditions. It can be seen that numerical-based $| I_v |$ correspond reasonably well with the analytical values by Mylonakis and Gazetas [9]. In higher frequency ratios, the values decrease significantly, showing higher filtering against the vertical dynamic waves with more height of the soil domain.

In Fig. 8, $| I_v |$ based on elastic soil are related to the resulting values by elastic soil with the soil-pile interface, nonlinear soil only, and nonlinear soil with the soil-pile interface. In contrast to the irrelevance of consideration of soil-pile interface with elastic soil in RC-1, $| I_v |$ become relatively higher than those obtained by the elastic soil with floating pile-tip boundary conditions. Hence, the pile is able to translate more freely with constraints relying on the surrounding soil at the pile tip and pile shaft after facing the incoming vertical dynamic wave. With nonlinear soil, $| I_v |$ become higher than the ones attained from the elastic soil with soil-pile interface case due to lesser constraint to the vertical translation of pile. Moreover, the combination of soil and soil-pile interface nonlinearities allows a sharp increase in $| I_v |$; the values can reach around 2 in contrary to the reduction effect of vertical kinematic interaction with elastic soil considerations in the higher frequency region.

The resulting absolute amplification ratios ($| A |$) and phase differences (ϕ) for case RC-2 are plotted in Fig. 9. As experienced in the case of the end-bearing single pile, with the inclusion of nonlinearities, the pile movement amplifies against the applied oscillations at the soil base. Besides the maximum values near the first resonant frequency of the soil, the decrease in values by the filtering process in higher frequencies can be seen. Moreover, the difference in pile movement by each numerical case becomes more noticeable in higher loading frequency ranges. Furthermore, higher values of ϕ can be noticed in the case of the floating pile, due to the presence of sufficient soil depth beneath the pile tip. Overall, the values of ϕ between the pile top oscillation to soil base oscillation does not vary much with nonlinearities.
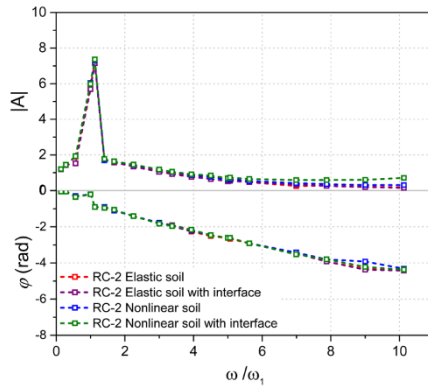
Fig. 9: Amplification ratio and corresponding phase at pile-top of floating single pile.
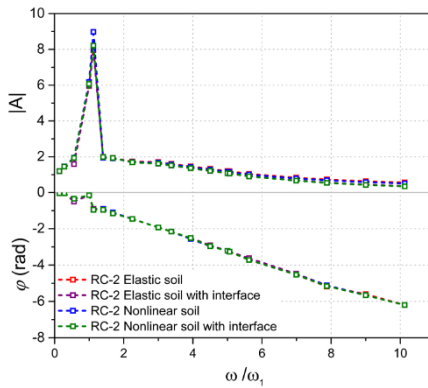

Fig. 10: Amplification ratio and corresponding phase at soil surface of floating single pile.

The amplification ratios (| A |) based on the ratios of oscillations achieved at the soil surface to those applied at the soil base are summarised in Fig. 10. After the maximum amplification at the first resonant frequency, a decrease in values can be observed. The filtering ability of soil against higher frequency components of the dynamic loading is maximum in the case of nonlinear soil with the soil-pile interface. Hence, the ratios of the decreasing values of amplification at the soil surface to the increasing values at the pile top (i.e., Fig. 9) result in a dominant increase of kinematic interactions (i.e., Fig. 8). Also, higher values of damping in the soil are observed due to higher soil depth.

4. Conclusion

This study investigates the effect of soil and soil-pile interface nonlinearities on vertical kinematic interactions of piles. For this purpose, numerical modelling using three-dimensional finite elements was used. Two kinds of piles are analysed: end-bearing single pile and floating single pile. At first, the kinematic response factors for the end-bearing single pile are validated with the past analytical/numerical-based studies using elastic soil. Then, by considering the soil-pile interface for elastic soil, it is confirmed that the kinematic interaction remains almost the same. While with nonlinear soil only or with the combination of nonlinear soil and soil-pile interface, the kinematic interactions can increase significantly due to an increase in the pile movement by lesser restraint offered by the surrounding weaker soil. Corresponding results of amplification at pile top and soil surface also highlight this finding.

In the case of floating single pile, the kinematic interactions by elastic soil with the soil-pile interface can be slightly higher than without it. This results from lesser constraint offered by the soil beneath the pile tip than the end-bearing conditions. The kinematic interactions increase with the inclusion of nonlinearities. Moreover, with amplification data at pile top and soil surface, it is clear that with nonlinearities, pile movement can increase while the soil surface movement can decrease, resulting in a significant rise in kinematic interactions.

It must be noted that the determined results are based on specific properties of soil and pile.

References

[1] N. Makris, G. Gazetas, and E. Delis, "Dynamic soil—pile—foundation—structure interaction: records and predictions.," Géotechnique, vol. 46, no. 1, pp. 33-50, 2009.

[2] U. Zafar, C. S. Goit, and M. Saitoh, "Experimental and numerical investigations on vertical dynamic pile-to-pile interactions considering soil and interface nonlinearities," Bulletin of Earthquake Engineering, 2021/07/22 2021.

[3] K. Fan, G. Gazetas, A. Kaynia, E. Kausel, and S. Ahmad, "Kinematic seismic response of single piles and pile groups.," Journal of Geotechnical Engineering, vol. 117, no. 12, pp. 1860-1879, 1991/12/01 1991.

[4] M. Kavvads and G. Gazetas, "Kinematic seismic response and bending of free-head piles in layered soil," Géotechnique, vol. 43, no. 2, pp. 207-222, 1993.

[5] R. M. S. M. S. Maiorano, L. S. d. Sanctis, S. Aversa, and A. Mandolini, "Kinematic response analysis of piled foundations under seismic excitation," Canadian Geotechnical Journal, vol. 46, no. 5, pp. 571-584, 2009.

[6] M. Faghihnia Torshizi, M. Saitoh, G. M. Álamo, C. S. Goit, and L. A. Padrón, "Influence of pile radius on the pile head kinematic bending strains of end-bearing pile groups," Soil Dynamics and Earthquake Engineering, vol. 105, pp. 184-203, 2018/02/01/ 2018.

[7] M. S. Ullah, H. Yamamoto, C. S. Goit, and M. Saitoh, "On the verification of superposition method of kinematic interaction and inertial interaction in dynamic response analysis of soil-pile-structure systems," Soil Dynamics and Earthquake Engineering, vol. 113, pp. 522-533, 2018/10/01/ 2018.

[8] G. Anoyatis, R. Di Laora, and G. Mylonakis, "Axial kinematic response of end-bearing piles to P waves," International Journal for Numerical and Analytical Methods in Geomechanics, vol. 37, no. 17, pp. 2877-2896, 2013.

[9] G. Mylonakis, "Kinematic Pile Response to Vertical P-wave Seismic Excitation," Journal of Geotechnical and Geoenvironmental Engineering, vol. 128, 10/01 2002.

[10] A. J. Papazoglou and A. S. Elnashai, "Analytical and field evidence of the damaging effect of vertical earthquake ground motion.," Earthquake Engineering and Structural Dynamics, vol. 25, no. 10, pp. 1109-1137, 1996.

[11] D. Dai, M. H. El Naggar, N. Zhang, and Y. Gao, "Kinematic response of an end-bearing pile subjected to vertical P-wave considering the three-dimensional wave scattering," Computers and Geotechnics, vol. 120, p. 103368, 2020/04/01/ 2020.

[12] F. Ji and R. Y. S. Pak, "Scattering of vertically-incident P-waves by an embedded pile," Soil Dynamics and Earthquake Engineering, vol. 15, no. 3, pp. 211-222, 1996/04/01/ 1996.

[13] Plaxis, PLAXIS- CONNECT Edition V21.00- reference manual. The Netherlands: Plaxis bv, Bentley Systems, Incorporated, 2020.